Neutron-wave-interference experiments with two resonance coils

S. V. Grigoriev,[1,2,*] W. H. Kraan[1], F. M. Mulder,[1] and M. Th. Rekveldt[1]
[1]*Interfacultair Reactor Instituut, TU-Delft, 2629 JB Delft, The Netherlands*
[2]*Petersburg Nuclear Physics Institute, Gatchina, St. Petersburg 188350, Russia*
(Received 22 February 2000; published 27 October 2000)

Neutron resonance spin-echo (NRSE) phenomena are investigated experimentally and theoretically. In our experiments, spin precession produced in a classical manner and by neutron resonance is combined as two arms of a spin-echo machine. A magnetic-field scan in the classical SE coil reveals a spin-echo signal of the precession produced by the NRSE arm. The neutron spin-flip probability ρ in the resonance coils turns out to be a key parameter of the NRSE arm. The limiting cases $\rho=0$ and $\rho=1$ lead, respectively, to Larmor precession with phase ϕ_1 in the static magnetic fields of the NR flippers *or* to NRSE precession with ϕ_2. The case $0<\rho<1$ produces quantum interference resulting in additional echoes with phases $\phi_3=(\phi_1+\phi_2)/2$ and $\phi_4=\pm(\phi_1-\phi_2)/2$. The amplitude of each pattern depends on the spin-flip probability ρ and the initial polarization. These experiments demonstrate explicitly the quantum-mechanical principle of linear spin state superposition of neutron particle waves, and the interference as a result of that.

PACS number(s): 03.75.Dg

I. INTRODUCTION

Spin-echo (SE) neutron spectroscopy, first introduced by Mezei in 1972 [1], has developed into a powerful method to determine the energy transfers in neutron beam scattering experiments. In this method the energy transfer or velocity change of neutrons caused by a sample is measured by comparing the Larmor precession in a well defined magnetic field before and after scattering. The strength and length of the magnetic field and the stability of the precession devices of the SE machine determine the resolution and accuracy of the SE experiment.

Though the SE technique is well established after nearly thirty years, a new development started when Gähler and Golub proposed an alternative possibility to produce spin precession in zero field (ZF precession) between two resonance spin flippers containing RF coils [2–4]. In a number of articles they investigated the main principles of the ZF precession and carried out experiments showing advantages and possibilities of the new ''mode'' in SE—spectrometry. The possibility to create this unusual precession in the ZF region between two RF spin flippers was first discussed in the works of Badurek [5,6] and Mezei [7]. It is based on understanding Larmor precession as an interference phenomenon between two superposed neutron waves. Mezei in his paper [7] explained that inside the static magnetic field region the incoming neutron wave with momentum $\vec{k}$ will become the superposition of spin state waves with a phase shift or polarization rotation angle, which is given by the momentum difference $\vec{k}_+$ and $\vec{k}_-$. There are other possibilities, besides a static magnetic field, to create a phase difference between neutron states. A pair of RF spin flippers can produce such a difference. Using the perfect crystal neutron interferometer, Badurek and co-workers [5,6] demonstrated that one can observe an interference pattern caused by RF spin flippers located in both arms of the interferometer. Later Gähler and Golub, experimenting with two RF spin flippers, developed neutron resonance spin echo (NRSE) as a new method in SE spectrometry. It must also be mentioned that an analogous phenomenon of interference between two waves was discussed by Ramsey in his resonance method of the separated oscillating fields [8,9]. He considered a beam with spin $\pm\frac{1}{2}$ particles (a two-level system) passing through these fields while being in resonance with the particle's magnetic moment. The transition probability between the levels was calculated. The calculations demonstrated the neutron wave interference between the two possible wave paths through spin-momentum space.

This paper contains a description and theoretical consideration of experiments with two RF spin flippers in which a partial rather than a complete spin-flip process occurs. This results in the appearance of four neutron waves in the space between flippers. These waves interfere and each pair of them produces a new distinct interference pattern. We will give a theoretical treatment of this problem. For simplicity one of the resonance conditions is considered to be fulfilled, i.e., the frequency of the RF field matches the Zeeman energy difference between the two spin eigenstates produced by the permanent field. In spite of this restriction, the solution contains all details arising from the partial spin-flip process, as one tunes the spin-flip probability from 0 to 1 by varying strength of the RF field. The formulas describing the appearance of four neutron waves in this double-resonance experiment are derived in Sec. II. Section III gives details concerning the setup. It contains elements of both the spin-echo technique and three-dimensional analysis of neutron polarization. The results of the measurements are given in Sec. IV.

II. PRECESSION AS INTERFERENCE BETWEEN PLANE NEUTRON WAVES

A. Precession in stationary field

Larmor precession may be understood quantum mechanically [7] by realizing that a plane neutron wave

*Email address: grigor@rvv.lnpi.spb.su

$\exp(ik_0x)\exp(-i\omega t)$ with initial wave number k_0 and energy $\hbar\omega$ is split into two plane waves with wave numbers k_+ and k_-, as soon as the neutron enters the field B. The wave is assumed to travel along the x axis, so the wave vector equals $(k_0,0,0)$; hence the wave is represented as $\exp(ik_0x)$. Due to the law of conservation of energy, the total energy $\hbar\omega$ does not change and these waves satisfy the equation

$$\frac{\hbar^2k_0^2}{2m_n}=\frac{\hbar^2k_+^2}{2m_n}-\mu_nB=\frac{\hbar^2k_-^2}{2m_n}+\mu_nB, \tag{1}$$

from which one finds k_+ and k_- in first approximation:

$$k_\pm=k_0\pm\frac{\mu_nB}{\hbar v}, \tag{2}$$

where m_n, μ_n, and v are the mass, the magnetic moment, and the velocity of the neutron, respectively.

At the end of the field at point $x=l$ the phases k_+x and k_-x of both plane waves have progressed by different amounts, but here the splitting into k_+ and k_- is lifted, so the phase difference stops to grow and is equal to $\phi=(k_+-k_-)l=(2\mu_n/\hbar v)Bl$. Because it is not explicitly necessary that the field is homogeneous along x but may depend on x, it is better to speak about the phase ϕ as an integral $\int_l[k_+(x)-k_-(x)]dx$. So the Larmor precession is presented as an integral over the difference in wave numbers of the split plane neutron waves.

B. Precession in time-dependent field

A few years ago, Golub and Gaehler demonstrated [2] that precession of a neutron spin may be effectively produced in the system of two RF spin flippers placed at a distance L from each other. If spin flipping occurs, the total energy of the neutrons is no longer conserved because of exchange of a photon of energy $\hbar\omega_{\mathrm{RF}}$ between the neutron state and the RF field. Its frequency is adjusted such that the photon energy exactly equals the Zeeman energy difference between the two spin eigenstates of the neutron in the static field, that is,

$$\hbar\omega_{\mathrm{RF}}=-2\mu_nB. \tag{3}$$

Depending on the strength B_{RF} of the RF field, the probability for the neutron to change its spin eigenstates, by absorbing or emitting a photon, can be changed between 0 and 1. During the spin flip in the RF field, neutron spin states with momenta k_+ and k_- will gain or lose an amount of potential energy $\Delta E=2\mu_nB$. Then, upon leaving the static field their potential energy is released as a kinetic energy change. The splitting of the wave vector is not lifted, but doubled: k_- becomes $k_{--}=k_0-(2\mu_nB/\hbar v)$; k_+ becomes $k_{++}=k_0+(2\mu_nB/\hbar v)$. In the zero-field region after the flipper these waves interfere and their phase difference $\phi=\int_0^x[k_{++}(x')-k_{--}(x')]dx'-2\omega_{\mathrm{RF}}t$ implies an effective precession in space. This spatial precession, however, takes place in zero field [so-called ''zero-field (ZF) precession'']. In a static experiment this is unobservable because the phase difference between the two interfering waves continues to grow in time at the rate $2\omega_{\mathrm{RF}}$. Nevertheless, such a nonstationary interference pattern exists and was observed for the first time by Badurek *et al.* [10] using stroboscopic neutron detection. The time-dependent behavior in ZF precession may be halted by transmitting the neutron through another RF spin flipper identical to the first one. Then both k_{++} and k_{--} return to k_0 and also the difference in evolution rate in time ω_{RF} disappears by emitting or absorbing the photon in the second flipper. Thus, the growth of both the spatial and time phase difference, i.e., the precession, is halted.

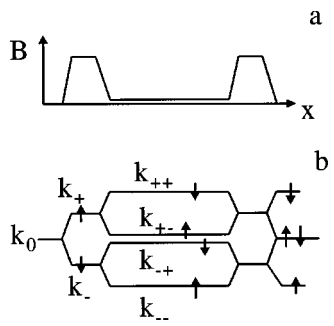

FIG. 1. (a) Sketch of the system of the magnetic fields of the two RF spin flippers with a guide field between them. (b) (k,x) diagram of the wave vectors as a function of position along the beam.

Figure 1(a) shows schematically the system of the magnetic fields of two RF spin flippers with the guide field between them. Figure 1(b) is the (k,x) diagram, i.e., diagram of four different wave-vector paths between the flippers as a function of position along the beam. The levels k_{++} and k_{--} represent the splitting in momentum when the spin-flip probability ρ of both flippers is equal to 1, while k_{+-} and k_{-+} appear when $\rho=0$, that is, RF power switched off. In this last case we return to the usual Larmor precession in the static magnetic fields of the flippers. However, when the resonance conditions are not fulfilled, thus ρ is less than 1, all neutron states represented by the lines in Fig. 1 really coexist and can be occupied by the same neutron. To observe their interference, contrary to earlier authors working in this field, we varied the flipping probability of our RF spin flippers by varying the amplitude of the RF field. This is a common practice in other resonance techniques, e.g., nuclear magnetic resonance.

Figure 2 is helpful to analyze the phase shift between pairs of neutron waves after leaving the second flipper. When the RF power is switched off, this phase shift is proportional to the shaded area I and equals $\phi_1=\int[k_{+-}(x)-k_{-+}(x)]dx$, where the integral is taken over the whole length of the two-flipper system. k_{+-},k_{-+} indicate the paths of the neutron waves split in the first flipper. This is referred to as ''DC'' precession, that is, Larmor presession in the static field of the flippers only. When RF power is switched on (spin-flip probability $\rho=1$) the amount of ZF precession is proportional to the shaded area II and is equal to $\phi_2=\int[k_{++}(x)-k_{--}(x)]dx$.

As noted earlier, when $0<\rho<1$ all four k levels in the space between flippers will be occupied by a neutron. The shaded areas III and IV in Fig. 2 correspond to phase shifts

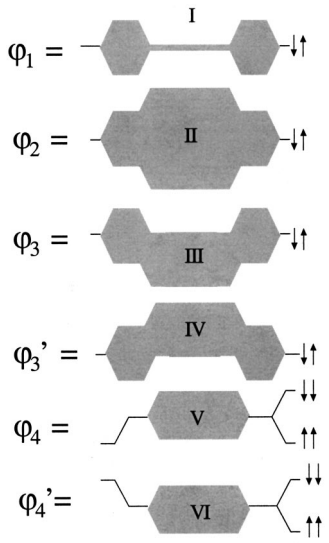

FIG. 2. The shaded areas show the phase shifts between pairs of the neutron waves after leaving the second flipper.

$\phi_3=\int[k_{++}(x)-k_{-+}(x)]dx$ and $\phi_3'=\int[k_{+-}(x)-k_{--}(x)]dx$. One can show that $\phi_3=\phi_3'=(\phi_1+\phi_2)/2$, so these interference ''terms'' correspond to half the ''sum area'' of I and II. The interference terms with $\phi_4=\int[k_{++}(x)-k_{+-}(x)]dx$ and $\phi_4'=\int[k_{-+}(x)-k_{--}(x)]dx$ correspond to the shaded area V and VI. They are also equal to each other and to half the ''difference area'' of II and I: $\phi_4=\phi_4'=(\phi_2-\phi_1)/2$. We will show that these two last terms are the interference patterns in Ramsey's problem of the separated oscillating fields [8,9].

The waves are not specified completely by plane waves as assumed above, since the state function contains also a spin part, which is the reason that all these waves actually appear. One can follow in Fig. 1 what happens to both spin states along the beam path. It is indicated at different positions in Fig. 1 by arrows $\uparrow$ and $\downarrow$, which correspond to the spinor components $\uparrow=\binom{1}{0}$ and $\downarrow=\binom{0}{1}$. Each k level between the flippers in diagram 1 can be identified by one spinor component only. Coefficients in the spinors accounting for the spin state of the initial wave and depending on the spin-flip probability of the flippers determine the occupation numbers of the neutron wave on each level, i.e., along each line in the diagram.

For the interference patterns I, II, III, and IV, the linear superposition of pairs of waves implies that initially the spinor components $\uparrow$ and $\downarrow$ are equally occupied. This means experimentally that the polarization corresponding to the Ist, IInd, IIId, and IVth terms is perpendicular to the quantization axis which we take to be the z axis. The areas V and VI are characterized by a sum of $\uparrow$ and $\uparrow$ spinors, so one of the spin states is not occupied, which implies that the polarization is parallel to the quantum axis z. Hence the interference pattern corresponding to the areas V and VI appears when one spin state is initially more occupied than the other. When both of them are initially equally occupied, the last pattern with $P\|z$ disappears but the other three terms with $P\perp z$ become observable.

C. Quantitative approach

In order to derive all these effects quantitatively, we have to treat the behavior of a plane neutron wave $\Psi(t_1)$ with initial occupation numbers at time $t_1\binom{\alpha(t_1)}{\beta(t_1)}$ in the system of two RF spin flippers separated in space by the distance L as a solution of the Schrödinger equation. Here t_1 is the time at which the neutron enters the first RF flipper. First we consider the wave of a neutron with velocity v passing through the first flipper of length l producing a static field B_0 and a transverse rotating magnetic field with frequency ω_0 and amplitude B_{RF}. The Schrödinger equation for this system can be written as

$$i\hbar\frac{d\Psi}{dt}=\begin{pmatrix}-\mu_n B_0 & \mu_n B_{\mathrm{RF}}\exp(i\omega_0 t)\\ \mu_n B_{\mathrm{RF}}\exp(-i\omega_0 t) & \mu_n B_0\end{pmatrix}\Psi(t). \tag{4}$$

When ω_0 satisfies the resonance condition (3), i.e., $\omega_0=\gamma_n B_0$ with $\gamma_n=-2\mu_n/\hbar$, its solution for a neutron leaving the system at a time $t_1+\tau$ (where $\tau=l/v$) can be written [8]

$$\Psi(t_1+\tau)=\begin{pmatrix}\cos(b\tau/2)\exp(i\omega_0\tau/2) & -i\sin(b\tau/2)\exp(i\omega_0(t_1+\tau/2))\\ -i\sin(b\tau/2)\exp(-i\omega_0(t_1+\tau/2)) & \cos(b\tau/2)\exp(-i\omega_0\tau/2)\end{pmatrix}\Psi(t_1)=\hat{C}(t_1,\tau)\Psi(t_1). \tag{5}$$

Here we introduced the designation $b=\gamma_n B_{\mathrm{RF}}$. Next the neutrons fly through a space L free of magnetic field. In this space they are not influenced by the magnetic field until they enter the second flipper at the moment $t_1+\tau+T$, where $T=L/v$. So only the time-dependent part of the spinor function is changed: $\Psi(t_1+\tau)$ becomes $\Psi(t_1+\tau+T)$. Finally upon leaving the second flipper at $t_1+\tau+T+\tau$ the neutron states may be described according to Eq. (5) by $\Psi(t_1+\tau+T+\tau)=\hat{C}(t_1+\tau+T,\tau)\Psi(t_1+\tau+T)$.

The spin-flip probability ρ of the RF flipper plays a ''key'' role in the distribution of the neutron wave over the different k levels in this double-resonance experiment. One can derive the expression for the spin-flip probability ρ from Eq. (5). Assuming the initial occupation numbers $\alpha(t_1)=1$ and $\beta(t_1)=0$, the spin-flip probability is given by the occupation number of the spinor component $\downarrow$ after the flipper:

$$\rho=\beta^*(t_1+\tau)\beta(t_1+\tau)=\sin^2(b\tau/2). \tag{6}$$

Hence ρ depends on the value of the amplitude b and time τ which is proportional to the neutron wavelength λ. So a dis-

tribution of the polarization over the two states is described by sin and cos functions of the argument $\beta\tau/2$. Equation (6) means that full spin-flip occurs for

$$b\tau=\pi. \tag{7}$$

In classical terms this means that the amplitude of the RF field, the length of the RF coil, and the neutron velocity should be matched such that a ''rotation of the polarization vector'' over π takes place during the neutron travel time through the RF coil.

Now we proceed to calculate the final polarization in the x,y,z directions using the resulting function $\Psi(t_1+\tau+T+\tau)$. The polarization component P_i is found by calculating $\langle\sigma_i\rangle=\Psi^*(t_1+\tau+T+\tau)\sigma_i\Psi(t_1+\tau+T+\tau)$, where σ_i is the (2×2) Pauli matrix for that polarization component. To produce results which can be compared with experiments, we need to specify the polarization state of the neutron beam before entering the first flipper. When we start with polarization along the y direction, the occupation numbers $\alpha(t_1)$ and $\beta(t_1)$ of the spinor components are both equal to $1/\sqrt{2}$.

The final polarization components are denoted P_{yx}, P_{yy}, and P_{yz} where the indices refer to the initial and final polarization components, successively. The polarization components in the x, y, and z directions consist of numerous terms. Most of them are oscillating functions of time t_1 and hence do not contribute to the time-averaged polarization as is measured in our experiments. We may therefore average out these terms obtaining for the polarization components P_{yx}, P_{yy}, and P_{yz}

$$P_{yx}=\langle\sigma_x\rangle=(1-\rho)^2\cos(2\omega_0\tau)+\rho^2\cos(2\omega_0(T+\tau))-2\rho(1-\rho)\cos(\omega_0(T+2\tau)), \tag{8}$$

$$P_{yy}=\langle\sigma_y\rangle=(1-\rho)^2\sin(2\omega_0\tau)+\rho^2\sin(2\omega_0(T+\tau))-2\rho(1-\rho)\sin(\omega_0(T+2\tau)), \tag{9}$$

$$P_{yz}=\langle\sigma_z\rangle=0. \tag{10}$$

In the above formulas, $\sin^2(b\tau/2)$ was substituted by the spin-flip probability ρ of one flipper [Eq. (6)] and $\cos^2(b\tau/2)$ was substituted by the spin-nonflipping probability $(1-\rho)$.

In Eqs. (8) and (9) one can see that when the spin-flip probability is not equal to 1, that is, for example, $0<b\tau/2<\pi/2$, three terms will be present in the P_{yx} and P_{yy} polarization components. The first term corresponds to the usual Larmor precession in the static magnetic field B_0 of the flippers and its phase is $\phi_1=2\omega_0\tau=2\gamma_nB_0l/v$. This is the interference of those parts of the neutron wave without spin flip in both the first and second flippers. Its amplitude is equal to $(1-\rho)^2$, i.e., the ''nonflipping'' probability in the two flippers. The second term in Eqs. (8) and (9) corresponds to the interference of the waves with spin flipped in each flipper. Its amplitude is equal to ρ^2 and its phase is $2\omega_0(T+\tau)$. It is the so-called ''zero-field precession'' [2–4]. The third term is the interference between those two. It is a superposition of the waves with spins flipped twice and not flipped. Its amplitude is the product of flipping and ''nonflipping'' probabilities $2(1-\rho)\rho$ while its phase is $\omega_0(T+2\tau)$. The phases of all these terms are drawn in Fig. 2 as the shaded areas I, II, III, and IV.

Starting with the initial polarization along the z direction [$\alpha(t_1)=1$ and $\beta(t_1)=0$], one can find for the final polarization components P_{zx}, P_{zy}, and P_{zz}

$$P_{zx}=\langle\sigma_x\rangle=0, \tag{11}$$

$$P_{zy}=\langle\sigma_y\rangle=0, \tag{12}$$

$$P_{zz}=(1-2\rho)^2-4\rho(1-\rho)\cos(\omega_0T). \tag{13}$$

The calculation of the polarization components P_{zx} and P_{zy} produces time-dependent terms only, which after averaging out, results in zero value of these polarization components. No term dependent on time appears in P_{zz} and it consists of two time-independent terms only. The first term in P_{zz} [Eq. (13)] corresponds to a spin-flip in each flipper and it approaches zero, when $b\tau=\pi/2$, that is, the spin-flip probability ρ equals $\frac{1}{2}$. It is trivial that its phase equals zero since there is no sinusoidal term. It is referred to as ''0 phase'' term. The second term is the one appearing in the Ramsey problem [8]. Its phase ω_0T corresponds to shaded area V in Fig. 2. The amplitude $4\rho(1-\rho)$ of this term is also a product of flipping and ''unflipping'' probabilities.

In the last calculation the initial polarization is parallel to the magnetic field, so only one spin state is initially involved (Fig. 2, the lowest scheme, upper part). There are two contributions to the final polarization P_{zz} coming from the waves being at the levels k_{++} and k_0. It is clear that the waves belonging to the same k level and the same spin state have no difference in total energy. Therefore, there is no evolution in time of their phase difference. Since two waves are present on each level, both pairs of waves after interference produce stationary patterns which are, in fact, intensity variations as a function of phase line integral ϕ_4. So the two intensities of both levels add up to ϕ_4-dependent polarization with independent total intensity. We notice that both interfering waves on the level k_{++} have the ''down'' spin state, i.e., the interference pattern has negative polarization. The two waves at the level k_0 with ''up'' spin state produce a pattern with positive polarization. Thus the probabilities R to find the neutron at the levels k_0 and k_{++} are given by

$$R(k_0)=\alpha^*(t_1+\tau+T+\tau)\alpha(t_1+\tau+T+\tau)=1-2\rho(1-\rho)[1+\cos(\omega_0T)], \tag{14}$$

$$R(k_{++})=\beta^*(t_1+\tau+T+\tau)\beta(t_1+\tau+T+\tau)=2\rho(1-\rho)[1+\cos(\omega_0T)]. \tag{15}$$

Their difference results in a polarization $P_{zz}=\alpha^*\alpha-\beta^*\beta$ and coincides with Eq. (13). In fact, the probability R changes as the cos function of the phase ω_0T, so when $R(k_0)=1$ at $\omega_0T=(2n+1)\pi$ (n is an integer number), then $R(k_{++})=0$ and vice versa at $\omega_0T=2n\pi$. As seen from Eqs. (14) and (15), their sum is always 1: $R(k_0)+R(k_{++})=1$.

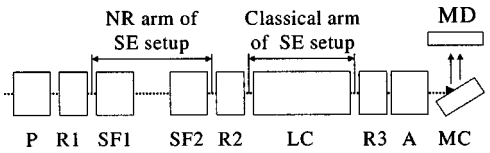

FIG. 3. Schematic drawing of the setup realized at the SP beam line at IRI Delft: *P*, polarizer; $R1$, $R2$, and $R3$, polarization rotators; SF1 and SF2 are the RF spin-flippers; LC, Larmor coil; *A*, analyzer; MC, monochromator crystal; MD, set of detectors for quasimonochromatic beams. The system consisting of SF1 and SF2 makes up the first arm of a spin-echo setup. The phase ϕ caused by the interference between any pair of neutron states is measured as the field B_1 generated in LC needed to compensate this phase. So the LC makes up the second arm of the spin-echo setup.

III. LAYOUT OF THE DOUBLE-RESONANCE EXPERIMENT

The measurements described in this paper were carried out using the polarizing mirror setup SP at IRI, Delft. Figure 3 gives a schematic outline of this setup. A polychromatic neutron beam emerging from a 2 MW swimming-pool type reactor is polarized by polarizer *P*. Using rotator ($R1$) the polarization of the beam can be successively rotated towards one of the laboratory axes j ($j=y,z$), i.e., parallel (z) or perpendicular (y) to the guide field. The system consisting of two RF spin flippers is located downstream this rotator $R1$. The two flippers can be considered as a first arm of a spin-echo setup. In our experiments we set the value of $B_0=99$ G and the frequency of the oscillating field 291 kHz, respectively, to fulfill the resonance condition Eq. (3). The length of the RF coils is 0.1 m and they are placed at a heart-to-heart distance of 0.4 m. After transmission through the two RF coil system, the polarization can be rotated again towards the axis j ($j=y,z$) by rotator $R2$. The second arm of the spin-echo setup is a block shaped coil [called ''Larmor Coil'' (LC)] of length 0.32 m which produces a static magnetic field $\vec{B}_1$. Its direction is opposite to the static magnetic field in the flippers $\vec{B}_0$. The ''Larmor coil'' is followed by a third polarization rotator ($R3$) and an analyzer (A). By Bragg reflection at a monochromator crystal (MC), neutrons are reflected into the neutron multidetector (MD). Since the MD has different scattering angles for the eight detectors, it allows us to simultaneously measure the spin-echo signal at eight different values of the neutron wavelength: $\lambda=0.190$, 0.204, 0.210, 0.220, 0.225, 0.232, 0.243, and 0.260 nm. The spread of the wavelength spectrum in each detector is 0.02 nm, approximately.

By suitable setting of $R1$, $R2$, and $R3$ we can measure P_{yy}, P_{zz}, P_{zy}, and P_{yz}, where the first and second indices indicate the initial and final polarization components. These polarization components are measured as a function of the phase ϕ. It is expressed by the value of the magnetic field B_1 in the ''Larmor coil'' which is necessary to compensate this phase ϕ collected by the spin in the first arm of the SE machine. So, in these experiments we unite three-dimensional polarization analysis and the spin-echo technique.

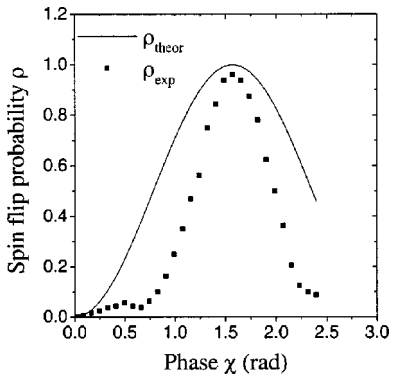

FIG. 4. Dependence of the spin-flip probability ρ in one RF flipper on the amplitude of the oscillating field B_{RF} at wavelength $\lambda=0.232$ nm: full line, Eq. (6); symbol, experiment described in Sec. IV A.

IV. RESULTS

A. Spin-flip probability

As was mentioned above, the spin-flip probability ρ is an important quantity that determines the amplitude of the SE signals in this double-resonance experiment. It was measured at $\lambda=0.232$ nm in a separate experiment with only one flipper between polarizer and analyzer by varying the amplitude of B_{RF}. In this setup one measures in fact P_{zz}. From the definition of the polarization, ρ is connected to P_{zz} by $\rho=(1-P_{zz})/2$.

Figure 4 shows the spin-flip probability ρ as a function of the phase $\chi=b\tau/2=\gamma_n B_{RF} l\lambda/2\beta$ with $\beta=v/\lambda$. It can be observed from Fig. 4 that the spin-flip probability has its maximum at $\chi=\pi/2$ and drops as the phase χ becomes bigger or smaller. The experimental function $\rho(\chi)$ differs strongly from the theoretical one given in Eq. (6), plotted with a full line. The difference between these two functions may be connected with the nonsharp boundaries of the magnetic field B_{RF} and B_0. In fact, the amplitude of the oscillating field B_{RF} decreases smoothly toward the ends of the RF coil. We will demonstrate in the next section that the amplitudes of the SE signals in our experiments are ruled by the experimentally measured spin-flip probability rather than by the theoretically expected one. In the experiments given below, the phase χ was varied by tuning b or the amplitude of the oscillating field B_{RF}. Additionally, the multidetector system MD (Fig. 3) allows one to vary χ by analyzing experiments at different neutron wavelengths.

B. Double-resonance experiment

The polarization as a function of the field B_1 in the second arm of the SE setup was measured at the different values of λ available and for several amplitudes of the oscillating field B_{RF}. Figure 5 shows the spin-echo signals at four different wavelengths when the RF coils are switched off ($B_{RF}=0$). So these SE signals correspond to Larmor precession in the magnetic field of the flippers B_0 (shaded area I in Fig. 2). It is seen that in order to compensate the phase ϕ in the first arm of the SE setup we need $B_1=125$ G. We indicate this with ''DC'' signal. The small fringes at the left side of the

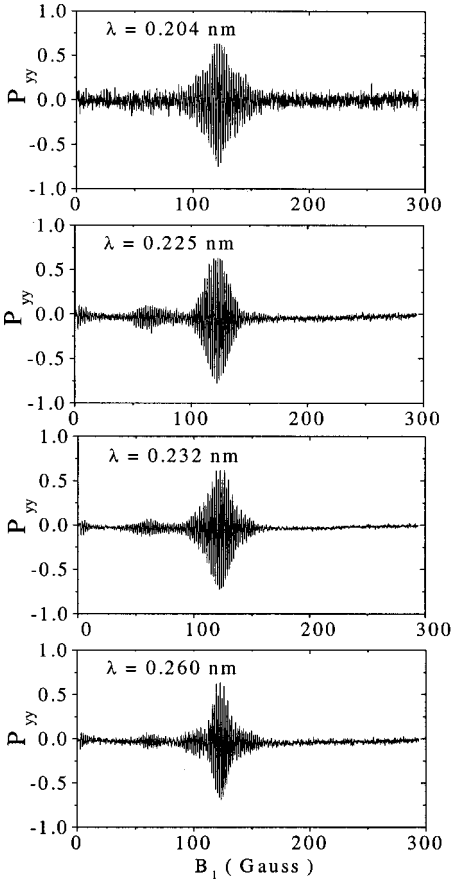

FIG. 5. Polarization P_{yy}: the spin echo signals at four different wavelengths as a function of the phase ϕ, i.e., as a function of the ''compensating'' field B_1 in the Larmor coil (LC in Fig. 3), when the RF coils are switched off: $B_{RF}=0$. This pattern is referred to as ''DC.''

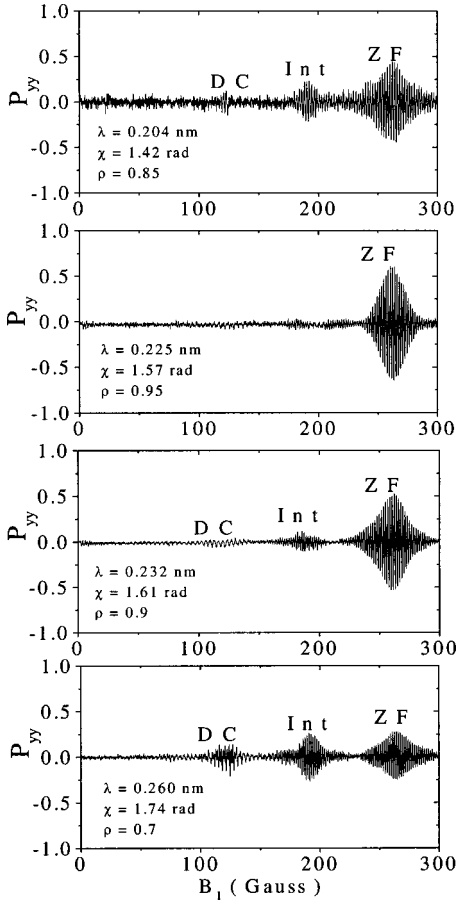

FIG. 6. Polarization P_{yy} as function of B_1, i.e., the spin-echo signal at four different wavelengths with $B_{RF}=3.0$ G. For this B_{RF} at these wavelengths the argument χ of Eq. (6) takes values such that $\rho\approx 0.85$ for $\lambda=0.204$ nm, $\rho\approx 0.95$ for $\lambda=0.225$ nm, $\rho\approx 0.9$ for $\lambda=0.232$ nm and $\rho\approx 0.7$ for $\lambda=0.260$ nm. The patterns marked ''DC,'' ''Int,'' and ''ZF'' refer to the corresponding terms in Eqs. (8) and (9).

main signal appear because of the presence of two slightly different wavelengths with different amplitudes in the wavelength spectrum.

Figure 6 shows the SE signals for four different wavelengths at an RF amplitude $B_{RF}=3$ G. The phases χ of the flippers according to Eq. (6) are mentioned in the figures. For $\lambda=0.225$ nm, i.e., $\rho\approx 0.96$, the SE appears at the value $B_1=260$ G. It is marked ''ZF.'' For smaller values of ρ at both sides of $\chi=\pi/2$, additional patterns appear at the position of the DC pattern: at $B_1=125$ G (also found with RF power off) and halfway between positions of the DC and ZF patterns, i.e., $(125+260)/2\approx 190$ G. This is the pattern corresponding to the interference term in Eqs. (8) and (9), marked ''Int.''

The amplitudes of the patterns ''DC,'' ''Int,'' and ''ZF'' correspond nicely to the amplitudes $(1-\rho^2)$, ρ^2, and $2\rho(1-\rho)$ of the terms in Eqs. (8) and (9) with ρ equal to ρ_{exp}, plotted by the squares in Fig. 4. For instance, for $\lambda=0.232$ nm with the RF power switched off, we find $P_0=0.7$ (Fig. 5). With RF power on, the amplitude $B_{RF}=3$ G, we find from Fig. 4 $\rho\approx 0.9$. Then the polarization of the patterns ''DC,'' ''Int,'' and ''ZF'' will have the values $P_{DC}=(1-\rho)^2P_0\approx 0.01$, $P_{int}=2(1-\rho)\rho P_0\approx 0.11$, and $P_{ZF}=\rho^2P_0\approx 0.56$, respectively. In accordance with this calculation, no DC pattern is observed within the error bars at this wavelength. We note that for χ far away from $\pi/2$, at $\lambda=0.260$ nm the ''DC'' pattern appears again.

As it is pointed out in Sec. IV A, to change the spin-flip probability one can also change the amplitude of the oscillating field B_{RF} instead of λ. Figure 7 gives the patterns ''DC,'' ''Int,'' and ''ZF'' observed for $\lambda=0.232$ nm at amplitude B_{RF} equal to 3.0 G, 2.42 G, and 2.15 G, i.e., $\chi=1.57$ rad, 1.3 rad, and 1.12 rad, respectively. The experimental spin-flip probability ρ_{exp}, according to the points in Fig. 4, gives $\rho_{exp}=\frac{1}{3}$, $\frac{2}{3}$, and 0.96, respectively. Again, the measured amplitudes of the patterns (after reduction by $P_0=0.7$) correspond to the calculated ones using Eqs. (8) and (9).

To observe the SE signal corresponding to the areas V and VI in Fig. 2, we have to scan the polarization P_{zz} as a function of B_1. According to Eq. (13) in case $\rho\neq 1$ the SE signal appears with amplitude $4\rho(1-\rho)P_0$ and at the phase $(\phi_{ZF}-\phi_{DC})/2$. We indicate this SE signal as ''Ramsey'' term (''RT'') referring to the problem set and discussed by Ramsey [8,9]. Figure 8 gives SE signals at $B_{RF}=2.15$ G for

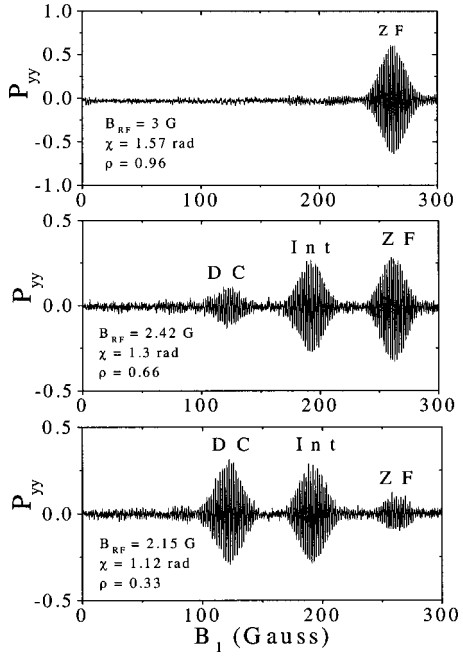

FIG. 7. Polarization P_{yy} as function of B_1, i.e., the spin-echo signal at three different values of B_{RF} and for the same wavelength $\lambda=0.225$ nm. For these B_{RF} at this wavelength the argument χ of Eq. (6) takes values such that $\rho\approx 0.96$ for $B_{\mathrm{RF}}=3.0$ G, $\rho\approx 0.66$ for $B_{\mathrm{RF}}=2.42$ G, and $\rho\approx 0.33$ for $B_{\mathrm{RF}}=2.15$ G. The patterns marked ''DC,'' ''Int,'' and ''ZF'' refer to the corresponding terms in Eqs. (8) and (9).

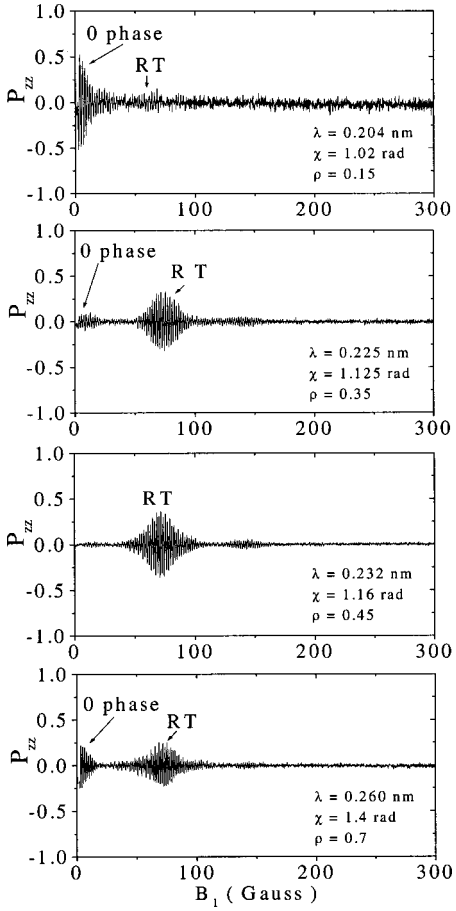

FIG. 8. Polarization P_{zz}: the spin echo signals at four different wavelengths with $B_{\mathrm{RF}}=2.15$ G, the positive axis of B_1. The amplitude 2.15 G of the RF field and observed wavelength determine the phase χ [Eq. (6)] such that the spin-flip probability ρ takes values $\rho\approx 0.1$ for $\lambda=0.204$ nm, $\rho\approx 0.3$ for $\lambda=0.225$ nm, $\rho\approx 0.45$ for $\lambda=0.232$ nm, and $\rho\approx 0.7$ for $\lambda=0.260$ nm. The patterns ''RT'' and ''0 phase'' refer to the corresponding terms in Eq. (13).

the different wavelengths which imply spin-flip probabilities $\rho=0.1$, 0.3, 0.4, 0.5, and 0.70, respectively (see Fig. 4). The position of this signal is just equal to half the difference between the DC and ZF patterns, i.e., $B_1=(265-125)/2=70$ G. The SE signal around $B_1=0$ (''0 phase'' term) at $\lambda=0.204$, 0.225, and 0.260 nm is well described by the first term of Eq. (13). It is absent at $\lambda=0.232$ because $\rho\approx\frac{1}{2}$ and then the amplitude of this term must be equal to 0.

The only puzzle is that the amplitude of the SE signal at ($B_1=70$ G) equals half the incident polarization, while the theory [Eq. (13)] predicts full polarization. This stimulated us to investigate the negative part of the phase scale, i.e., changing to negative values of the field B_1 in the ''Larmor'' coil. Indeed, we observed the second term with also half the magnitude of the initial polarization at $B_1=-70$ G (Fig. 9). An explanation of the phenomenon observed may be as follows. The polarization $\vec{P}$ obtained in the ''Ramsey'' experiment is an oscillating function of the phase ($\omega_0 T$): $\vec{P}_R=(0,0,P_0\cos(\omega T))$. It is shown in Eqs. (11)–(13) that only the component P_{zz} is not equal 0, while the time-averaged $P_{zx}=P_{yz}=0$. The oscillating z component of the polarization can be considered as a sum of the two counter-rotating polarization vectors with half initial amplitude each one. Thus, one can imagine the ''Ramsey'' pattern as a result of a rotation of the initial polarization P_z^0 in the two, opposite but coexisting, static magnetic fields, both of them being perpendicular to the z direction. We point out that this situation is fundamentally distinct from the case of the ''DC,'' ''Int,'' and ''ZF'' patterns. Then, according to Eqs. (8)–(10) the polarization is a rotating vector $\vec{P}_{\mathrm{DC,Int,RF}}=(P_0\sin(\phi),P_0\cos(\phi),0)$. The results of both experiments can be expressed by formulas in the following. The action of the ''Larmor'' coil with the magnetic field B_1 in the direction y on the polarization vector $\vec{P}=(P_x,P_y,P_z)$ can be described by the rotating operator:

$$\vec{P}'=\begin{pmatrix}\cos(B_1) & 0 & \sin(B_1)\\ 0 & 1 & 0\\ -\sin(B_1) & 0 & \cos(B_1)\end{pmatrix}\vec{P}_0. \qquad (16)$$

Actually, the rotating angle is equal to $\gamma_n B_1 l_c/v$, where l_c is the length of the ''Larmor'' coil, but for simplicity we omit the factors and say simply B_1. In case of Ramsey's experiment we have for $\vec{P}_0$ the vector $\vec{P}_R=(0,0,P_0\cos\phi)$ mentioned above. Applying the rotation operator to this polarization vector one gets $P_x'=P_0\sin(B_1)\cos(\phi)$, $P_y'=0$, and $P_z'=P_0\cos(B_1)\cos(\phi)=(1/2)P_0[\cos(\phi+B_1)+\cos(\phi-B_1)]$, i.e., this results in two SE signals with half amplitudes and

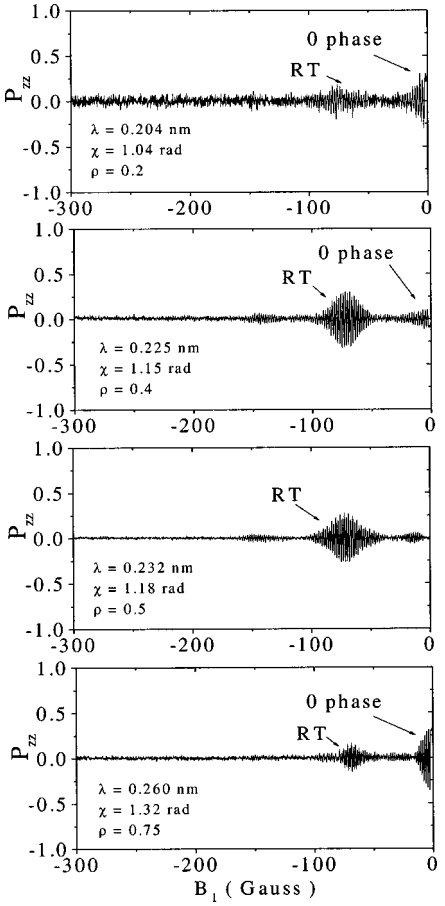

FIG. 9. Polarization P_{zz}: the spin echo signals at the four different wavelengths with $B_{\mathrm{RF}}=2.20$ G, the negative axis of B_1.

phases $B_1=\pm\phi$. When we substitute $\vec{P}_{\mathrm{DC,Int,RF}}$ for $\vec{P}_0$ in Eq. (16) with rotation operator of the magnetic field B_1 in the z direction [exchange y and z elements in rotation operator in Eq. (16)], we find $P_x'=P_0\cos(B_1)\sin(\phi)+P_0\sin(B_1)\cos(\phi)=P_0\sin(B_1-\phi)$, $P_y'=-P_0\sin(B_1)\sin(\phi)+P_0\cos(B_1)\cos(\phi)=P_0\cos(B_1-\phi)$, and $P_z'=0$. As is seen from the formulas, the oscillating polarization vector results in two SE signals with $\phi=\pm B_1$ and half-amplitude. In contrast, the rotating polarization finds its ''echo'' at only one magnetic field $\phi=B_1$.

C. Classical ''rotating-frame'' approach

Finally, it should be noted that the discussion above is not sufficient yet to explain the finding of two separated echoes in Ramsey's experiment since for a single wavelength the oscillations as a function of B_1 add constructively yielding only one observable oscillation over negative and positive B_1 values. However, since the monochromator produces a certain wavelength spread, a damping of the echo signal occurs for B_1 values far from the echo.

It is illustrative to describe this facet in a classical picture such as it is often applied in for instance nuclear magnetic resonance: a description in terms of precession relative to a rotating frame. As will become evident, this is especially useful for describing effects that are related to experimental neutron beams that have a finite wavelength spread.

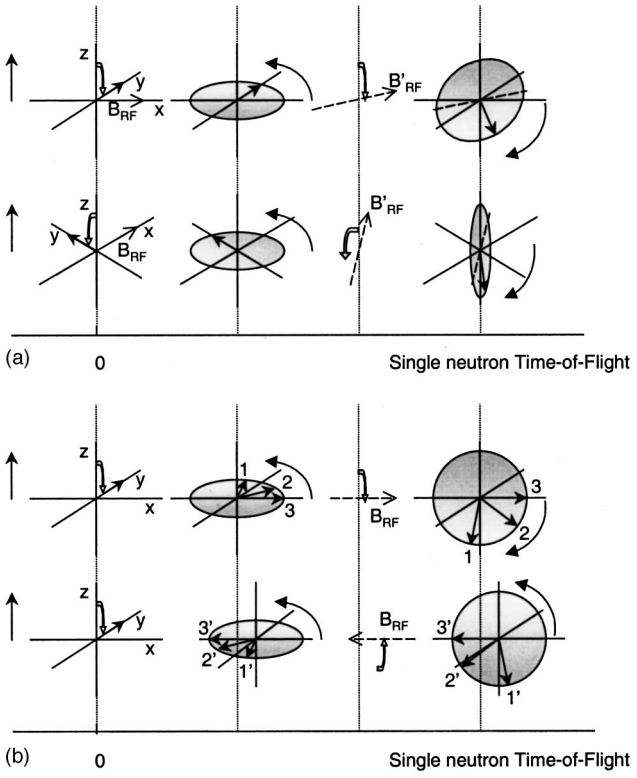

FIG. 10. (a) Effective action of the two flippers on a neutron spin described in a rotating frame picture. The rotating frame is defined with the z axis parallel to the applied static field in the flippers. For $\rho=\frac{1}{2}$, a spin initially along the z axis is rotated over 90° towards the $+y$ axis by the RF field (which is static in this rotating frame). The spin is rotated again 90° in a certain direction depending on the time spent between the flippers, i.e., depending on the neutron wavelength. A different arrival time at the first flipper is sketched below. (b) Effective precession relative to the rotating frame for two wavelength spectra that have wavelengths that are π out of phase relative to each other. Different wavelengths are indicated by three arrows having a slightly different precession relative to the rotating frame. Note that the effective sense of precession in the upper and lower part of the figure has different signs.

The static magnetic field of the flippers defines a frame that rotates with the Larmor frequency of the polarized neutron spins (the ''rotating frame''). The RF field has a frequency exactly matched to it and can therefore be described by a static magnetic field perpendicular to the z axis in this rotating frame. The neutron spin entering the first neutron flipper defines the time $t=0$ and the spin is taken to be parallel to the $+z$ axis. During the stay in the flipper the RF field rotates the spin towards the $+y$ axis; this defines the $+y$ axis of the rotating frame. When the neutron leaves the flipper there is no magnetic field left, and therefore the spin classically does not precess. However, the phase of the rotating frame defined above can still be followed. In Fig. 10(a) this is indicated by the arrow that gives a certain rotation of the rotating frame relative to the spin. Depending on the velocity (wavelength) of the neutron it arrives at the sec-

ond flipper at a time L/v later. The spin encounters the same magnetic field strength and in this field the spin will precess again with the Larmor frequency equal to the rotating frame frequency. However, the phase of the rotating frame encountered there is of importance, since the phase of the RF field is directly coupled to it. As is indicated in the figure, there is a certain static angle between the rotating frame and the RF field of the second flipper. It is this angle that determines the spin rotation by the second RF field.

For a neutron beam with a certain spread in wavelengths there will be a distribution in the times T and therefore the direction of the RF field relative to the rotating frame (or the phase of the RF field) will have a distribution of values. In Fig. 10(b) this is indicated by the circle and three different spin vectors with slightly different wavelengths. The different rotations define the effective precession in a sense that is the same for all these spins. After rotation in the second flipper the direction of this precession is conserved. However, when observing the different wavelengths one can state that neutrons that have time-of-flight values of T and of $T+(\pi/\omega_0)$, respectively, will encounter RF fields that are π out of phase. The effective resulting precessions in the rotating frame after the second flipper will have opposite signs therefore for this wavelength spectrum.

The neutrons arrive at different times at the first flipper, so the orientation of the rotating frame is changing at a rate ω_0 with respect to the laboratory frame [lower part of Fig. 10(a)]. In this picture it is for this reason that in the laboratory frame the effective precession between the flippers only yields a z component that is time independent. This was already noted above after the Eqs. (11) and (12). If, however, all neutrons would arrive at the same time at the first flipper and would have exactly the same wavelength, there would be time-independent x,y polarization too. In effect, this classical description leads to similar results when compared to the quantitative description of the preceding paragraph. In an experiment as a function of time the x and y polarization should be observable. This could be realized in experiments performed with stroboscopic neutron detection [10].

In obtaining a spin echo in the second arm of the instrument the precession in the first arm has to be reversed. Since the wavelength spectra that are π out of phase have a different sense of precession, the applied field should be of positive sign for one and of negative sign for the other wavelength spectrum. This explains why two echoes with half-intensities can be observed: one for each wavelength spectra with opposite B values. Note in this respect the additional ''beatings'' in the polarization as a function of B farther away from the origin at ± 125 G. This indeed indicates that the wavelength spectrum has a ''fine structure'' as described (like a comb).

The situation for the other three oscillations (''DC,'' ''Int,'' and ''ZF'') in P_{yy} polarization is similar in the sense that the finite wavelength spread again causes the damping of the oscillations far from the echo and makes the separate echoes visible in that way.

V. SUMMARY

In this paper we give a theoretical description of polarized neutron double-resonance experiments. The particular case, when the resonance condition is fulfilled, is considered. The description shows clearly the appearance of four possible time-independent spin-echo signals as a result of the interference between neutron waves in such a system. We have introduced the spin-flip probability and the initial polarization as key parameters of this system. The phases of the SE signals observed are determined by up to eight interfering waves. The experimental data are well described by the proposed theoretical picture. It is also worth noticing that the prediction of Ramsey [8,9] for a polarized neutron beam was experimentally tested.

ACKNOWLEDGMENTS

This work is part of the research program of the ''Stichting voor Fundamenteel Onderzoek der Materie (FOM),'' which is financially supported by the ''Nederlandse Organisatie voor Wetenschappelijk Onderzoek (NWO).'' The work was partly supported by the INTAS foundation (Grant No. INTAS-97-11329). One of the authors (S.V.G.) thanks RFFR (Project No. 00-15-96814) and the Russian State Programme ''Neutron Research of the Condensed State.''

[1] F. Mezei, Z. Phys. **225**, 146 (1972).
[2] R. Golub and R. Gähler, Phys. Lett. A **123**, 43 (1987).
[3] R. Gähler and R. Golub, J. Phys. (Paris) **49**, 1195 (1988).
[4] R. Golub, R. Gähler, and T. Keller, Am. J. Phys. **62**, 779 (1994).
[5] G. Badurek, H. Rauch, and D. Tuppinger, Phys. Rev. A **34**, 2600 (1986).
[6] G. Badurek, H. Rauch, and J. Summhammer, Physica B **151**, 82 (1988).
[7] F. Mezei, Physica B **151**, 74 (1988).
[8] N.F. Ramsey, Phys. Rev. A **48**, 80 (1993).
[9] N. F. Ramsey, *Molecular Beams* (Oxford University Press, Oxford, 1990).
[10] G. Badurek, H. Rauch, and J. Summhammer, Phys. Rev. Lett. **51**, 1015 (1983).